Carbohydrate Intramolecular Hydrogen Bonding Cooperativity and Its Effect on Water Structure

Jennifer L. Dashnau,* Kim A. Sharp, and Jane M. Vanderkooi

Johnson Research Foundation, Department of Biochemistry and Biophysics, School of Medicine, University of Pennsylvania, Philadelphia, Pennsylvania 19104

Received: August 3, 2005; In Final Form: October 5, 2005

Molecular dynamics (MD) simulations combined with water−water H-bond angle analysis and calculation of solvent accessible surface area and approximate free energy of solvation were used to determine the influence of hydroxyl orientation on solute hydration and surrounding water structure for a group of chemically identical solutes—the aldohexopyranose sugars. Intramolecular hydrogen bond cooperativity was closely associated with changes in water structure surrounding the aldohexopyranose stereoisomers. The OH-4 group played a pivotal role in hydration as it was able to participate in a number of hydrogen bond networks utilizing the OH-6 group. Networks that terminated within the molecule (OH-4 → OH-6 → O-5) had relatively more nonpolar-like hydration than those that ended in a free hydroxyl group (OH-6 → OH-4 → OH-3). The OH-2 group modulated the strength of OH-4 networks through syndiaxial OH-2/4 intramolecular hydrogen bonding, which stabilized and induced directionality in the network. Other syndiaxial interactions, such as the one between OH-1 and OH-3, only indirectly affected water structure. Water structure surrounding hydrogen bond networks is discussed in terms of water−water hydrogen bond populations. The impact of syndiaxial versus vicinal hydrogen bonds is also reviewed. The results suggest that biological events such as protein-carbohydrate recognition and cryoprotection by carbohydrates may be driven by intramolecular hydrogen bond cooperativity.

I. Introduction

Carbohydrates are ubiquitous in biology; nearly half of all proteins and lipids contain some form of glycosylation.[1] The carbohydrates found in glycoproteins and glycolipids are involved in a wide range of processes from molecular recognition and cell signaling[2] to protein stabilization and cryoprotection.[3] Although the chemical composition within a class of monosaccharides, such as the aldohexopyranose sugars, is identical ($C_6H_{12}O_6$), the orientation of hydroxyl groups can differ across stereoisomers (Figure 1). It is this subtle variation in hydroxyl orientation that is thought to account for differences in chemical and physical properties of the sugars − presenting a possible mechanism that would explain the diverse functional activity of these biologically relevant molecules.

The high hydroxyl (OH) content of carbohydrates is important to consider when explaining the interactions these molecules make with proteins and solvent. Arrangement of hydroxyl groups into intramolecular H-bond networks can lead to a phenomenon known as cooperativity.[4,5] Under cooperativity, directionally arranged H-bonds that form an H-bond network can increase the strength of individual H-bond donor or acceptor components. For instance, the H-bond formed between proton donor A−H and proton acceptor B will become stronger when an additional H-bond is formed between A*−H* and A−H to form the network A*−H* → A−H → B.

Cooperativity of carbohydrate intramolecular H-bond networks has been shown to influence the ability of these molecules to interact with other molecules such as pyridine.[5] These results have implications for understanding how carbohydrates interact with protein receptors in molecular recognition. Carbohydrates can also interact with the solvent itself, as is seen in the ability of these molecules to act as cryoprotectants in cold-tolerant organisms.[6] Therefore, there is a need to understand how H-bond cooperativity influences solute−solvent interactions and water structure.

In aqueous solution, solute structure has been shown to influence the structural, dynamic, and thermodynamic properties of surrounding water molecules.[7−9] However, experimental approaches have been only moderately successful at determining the precise details of such solute-induced water structuring. The commonly used techniques of neutron or X-ray scattering of liquids, while appropriate for study of ions and rare gases, are difficult to apply to complex solutes where spherically averaged data leads to loss of structural information.[10] Additionally, the high hydroxyl content of carbohydrates makes study by infrared spectroscopy (IR) difficult without using complex structural analogues. This difficulty is due to problems in deconvoluting contributions of solute and solvent in the OH stretching region as well as the strength of this region which often forces the intensity of the modes off scale. However, computer simulation can be used to effectively model solvent structuring around a solute.

In this work, theoretical methods are used to determine the impact of aldohexopyranose hydroxyl orientation on water structure. Analysis of molecular dynamics simulation of solvated sugars is performed using the technique developed by Sharp et al.[11−14] This technique, along with solvent accessible surface area and approximate solvation energy analysis, can be used to track how certain portions of a carbohydrate, such as the hydroxyl groups, influence the structure of surrounding water molecules.

* To whom correspondence should be addressed: jdashnau@mail.med.upenn.edu

10.1021/jp0543072 CCC: $30.25
Published on Web 11/23/2005

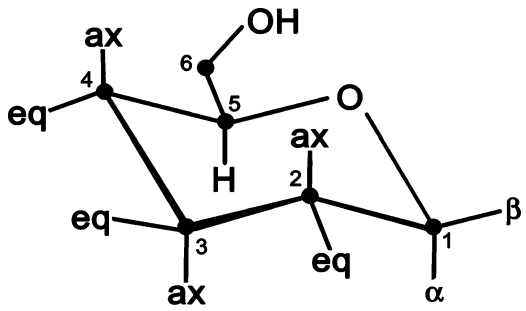

Monosaccharide	*OH-2*	*OH-3*	*OH-4*
Glucose	eq	eq	eq
Mannose	ax	eq	eq
Allose	eq	ax	eq
Galactose	eq	eq	ax
Altrose	ax	ax	eq
Talose	ax	eq	ax
Gulose	eq	ax	ax
Idose	ax	ax	ax

Figure 1. General structure of the six-carbon aldopyranose sugars. The table lists the configuration of hydroxyl groups at carbon positions 2 through 4 with "ax" representing axial and "eq" representing equatorial.

II. Methods

A. Molecular Dynamics Simulations. Initial structures of the eight D-aldohexopyranoses in both α and β anomeric forms were based on the lowest energy B3LYP/6-31G** minimized coordinates of Ma, Schaefer, and Allinger.[15] For each simulation, a single-solute molecule was inserted into the center of a periodic 30 Å^3 box containing well-equilibrated TIP3P[16] water. The size of the box allows for more than three solvation shells surrounding the solute in the primary cell. All water molecules within 1.7 Å of the solute were removed and the system consisting of one solute molecule and roughly 900 water molecules was minimized using a sequence of three steepest-descent (SD) minimizations with decreasing harmonic solute constraints (100 steps each) followed by 200 steps of adopted-basis Newton−Raphson (ABNR) minimization with no solute constraints.

All simulations were performed with the molecular mechanics program CHARMM v.27b2[17] using the CHARMM-type carbohydrate parameters developed by Kuttel, Brady, and Naidoo.[18] The system was equilibrated for a total of 50 ps followed by production dynamics simulations run for a total of 1 ns. Equilibration and dynamics were performed using the Verlet integrator in steps of 2 fs at constant temperature and pressure of 300 K and 1 atm, as controlled by Nosé-Hoover dynamics[19−21] and the extended system piston method for temperature and pressure, respectively. Chemical bonds involving hydrogen atoms were constrained using the SHAKE algorithm.[22] A nonbond cutoff of 12 Å was used, and nonbond interactions were decreased to zero between distances of 10 and 11 Å by applying a switching function. Additionally, cubic periodic boundary conditions with the minimum image convention were employed to replicate water atoms to prevent artifacts introduced from a solvent boundary.

B. Analysis of Water−Water Angle Distributions and Intramolecular H-Bonds. Following production of the 1 ns trajectory, PRAM,[23] a program developed by the Sharp group, was used for analysis of solute hydration within the first solvation shell. Solute atoms were first classified according to partial charge: atoms were considered nonpolar if their partial charge magnitude was less than 0.35 and polar if it was greater than or equal to 0.35. Water molecules were then classified as first shell if they were within the first hydration shell of any solute atom type, i.e., within 5.6, 3.4, 3.6, or 5.3 Å of a C, O, N, or S atom, respectively. The distribution of water−water H-bond angles (θ) (Figure 2) between pairs of waters in the first solvation shell separated by less than 5 Å was then calculated for each saved frame of the trajectory. The H-bond angle distributions, $P(\theta)$, were separately accumulated according to the type of solute atoms inducing the structure. For example, for a water pair, if one of the water oxygen atoms was closest to a nonpolar solute atom and the other was closest to a polar solute atom, the H-bond angle was classified as part of the nonpolar−polar (mixed) distribution. The other two possible classes, nonpolar−nonpolar (nonpolar) and polar−polar (polar) distributions were also calculated. The areas beneath the two water−water angular distribution peaks A1 (low angle, centered at 12°) and A2 (high angle, centered at 52°) were then quantified by integration in Origin v.6 (OriginLab, Northampton, MA) and the ratio of the areas, A1/A2, was used to compare the hydration across solutes. Figure 3 illustrates representative $P(\theta)$ distributions.

Intramolecular H-bonding within the carbohydrate molecule was also monitored over the trajectory. An intramolecular H-bond was considered present within the saved frame of the trajectory if the distance between the hydrogen of one hydroxyl and oxygen of another hydroxyl or the ring oxygen was less than or equal to 2.45 Å. This cutoff was chosen as it corresponds to the first minimum distance in the $g_{OH}(r)$ distribution function of glycerol—a simple model for extensively hydroxylated molecules.[24] The frequency of intramolecular H-bonding for

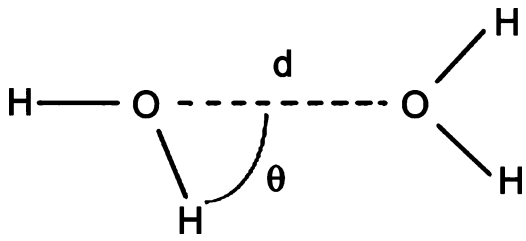

Figure 2. Water−water hydrogen bond angle (θ) and oxygen−oxygen distance (d).

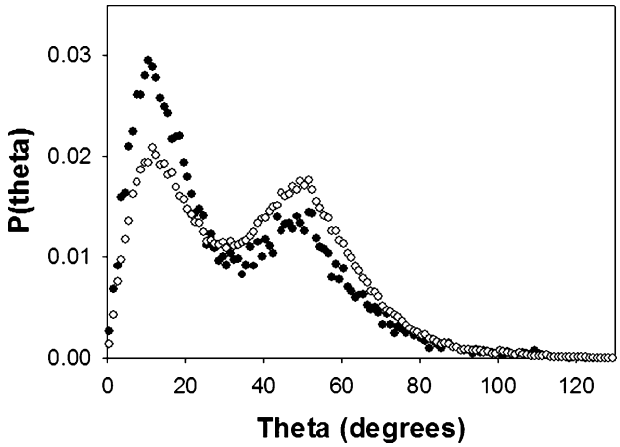

Figure 3. Water−water H-bond angle (θ) distributions surrounding nonpolar (solid circles) and polar (open circles) atoms of β-D-glucose.

each possible pair of hydroxyls was accumulated and used to understand effects of intramolecular H-bonding on water structure.

The sixteen aldohexopyranoses provide enough information to perform a full-factorial analysis of variance (ANOVA) to determine the significance of hydroxyl position to a particular response, for example, A1/A2 ratios. Minitab v.12 (Minitab, Inc., State College, PA) was used for ANOVA. Initially, first and second order terms were considered for the analysis (here referred to as "primary ANOVA"). Hydroxyl positions or interactions were deemed to have a significant correlation with response if probability values (P values) were less than or equal to 0.05. However, it should be noted that this cutoff is arbitrary and that P values indicate the probability that a given result occurred by chance rather than as a result of the treatment. Therefore, smaller P values indicate a smaller chance that a given result is obtained randomly. An additional run of ANOVA ("secondary ANOVA") was performed to examine the influence of main effects only on a response in the following circumstances: (A) when no second-order interactions were significant to the 0.05 level, or (2) when main effects or second-order terms were close to the 0.05 cutoff. The inclusion of second-order interaction terms in the error degrees of freedom can clarify the significance of main order effects.

To visualize how solute structure influences surrounding water structure, the average water−water H-bond angles formed by water molecules in the first solvation shell were mapped to their corresponding solute atoms. For clarity, only polar and nonpolar classes of water−water angles were mapped. The mixed class was omitted. As an example, the H-bond angle between two water molecules would be assigned to the nearest atoms associated with each of the water molecules. If water molecule 1 was closest to atom A and water molecule 2 was closest to atom B, then the water−water H-bond angle X would be included in both the atom A and B averages. This mapping of a pairwise property to single atoms remains interpretable since atoms A and B are of the same class. This is the reasoning behind omission of the mixed class when projecting the water structure onto the solute for visualization. The molecules were then colored by average water−water angle ranging from 27° (blue) to 43° (red).

C. Calculation of Solvent Accessible Surface Area and Approximate Solvation Energies. The lowest energy B3LYP/6-31G** minimized aldohexopyranose structures of Ma, Schaefer, and Allinger[15] were used for analysis of solvent accessible surface area (SASA) and approximate solvation energy. To estimate the free energy of solvation of each solute, PARSEII partial charges were assigned to each atom using the procedure described in Yang and Sharp.[25] The electrostatic potential of each solute in water (dielectric 80) and vacuum (dielectric 1) was determined by solving the Poisson−Boltzmann equation using the DelPhi application Qnifft.[26,27] The total solvent accessible surface area of each solute, calculated using the methods of Sridharan, Nicholls, and Sharp,[28] was used to determine the energy arising from the hydrophobic penalty. The total approximate free energy of solvation is the sum of electrostatic and hydrophobic penalty contributions. The influence of hydroxyl group position on solvent accessible surface area and solvation energy were analyzed by ANOVA through methods described above.

To visualize the effect of hydroxyl orientation on electrostatics, the electrostatic potential maps created by Qnifft[26,27] were displayed in PyMOL.[29] The contour values of the positive (blue) and negative (red) electric field isosurface contours were set at 0.25 and −0.25 kT/e, respectively. For the purpose of comparison, the sugars in this paper are shown in an orientation looking down on the sugar ring with the ring oxygen in the top center and carbon numbering ascending clockwise around the ring unless otherwise stated.

TABLE 1: Calculated Polar and Nonpolar Contributions to Aldohexopyranose Surface Area, Ranked by % Polar Area

sugar	configuration	number of axial OH	total area (Å^2)	% polar
α-D-idose	1a2a3a4a	4	304.72	57.90
α-D-talose	1a2a3e4a	3	308.46	59.19
α-D-gulose	1a2e3a4a	3	308.87	59.36
β-D-talose	1e2a3e4a	2	310.87	60.10
β-D-gulose	1e2e3a4a	2	310.84	61.87
α-D-galactose	1a2e3e4a	2	311.71	62.57
α-D-allose	1a2e3a4e	2	312.92	62.78
β-D-idose	1e2a3a4a	3	314.15	63.02
α-D-altrose	1a2a3a4e	3	310.96	63.15
β-D-galactose	1e2e3e4a	1	313.91	63.57
β-D-mannose	1e2a3e4e	1	317.04	64.59
β-D-altrose	1e2a3a4e	2	315.87	64.88
β-D-allose	1e2e3a4e	1	317.12	65.21
α-D-mannose	1a2a3e4e	2	312.25	65.60
α-D-glucose	1a2e3e4e	1	318.61	65.65
β-D-glucose	1e2e3e4e	0	320.06	66.83

III. Results and Discussion

A. Structural Changes Induced by Hydroxyl Orientation Affect Solute Hydration. Hydroxyl orientation and intramolecular H-bonding influence the structural properties of the aldohexopyranose stereoisomers. Equatorial hydroxyl configuration increases the total surface area accessible to solvent, or SASA (Table 1). When in equatorial configuration, hydroxyls are separated from the solute faces, where intramolecular H-bonding is more prevalent, to the periphery, where hydroxyls interact instead with solvent molecules. Thus, total SASA increases as the separation of the hydroxyls exposes surface area otherwise inaccessible to solvent during intramolecular H-bonding. This effect was seen earlier in molecular dynamics simulations by Brady, et al. in which anisotropic solvent structuring by the anomeric (OH-1) D-xylopentose hydroxyl group was investigated.[30] In their study, the α-anomer of D-xylopentose formed internal H-bonds with other hydroxyls, while the β-anomer formed H-bonding interactions with the surrounding solvent.[30] Increased SASA of the β-anomer was thought to improve H-bonding of this group to surrounding solvent by reducing intramolecular H-bond interactions. Consequently, they posited that local water structure and solvation energy would also be influenced based on the position of this group. We show here that the role of hydroxyl orientation on total SASA is extended to include not only the anomeric position, but other hydroxyls as well. A summary of P values is presented later (Table 4).

While the configuration of all hydroxyl groups was correlated with changes in total SASA, the fraction of the SASA associated with high partial charge groups, in this case hydroxyls, tracks roughly with the total number of axial groups. The fraction of SASA associated with high partial charge atoms is smaller for sugars with a greater number of axial hydroxyls. This result is likely due to the relatively strong intramolecular H-bonds that form when certain hydroxyls are in axial configuration. As explained by Lopez de la Paz et al., syndiaxial H-bonds (axial on the same face of the sugar) are stronger, or more stable in solution, than vicinal (adjacent) H-bonds.[5] Additionally, cis-vicinal (adjacent axial/equatorial) H-bonds are stronger than trans-vicinal (adjacent equatorial/equatorial) H-bonds. Therefore,

TABLE 2: Calculated Free Energy of Solvation (kcal/mol) for Aldohexopyranoses, Ranked by Total Free Energy

sugar	configuration	ΔG hydrophobic	ΔG electrostatic	ΔG total
α-D-idose	1a2a3a4a	2.304	−23.941	−21.637
β-D-talose	1e2a3e4a	2.322	−24.344	−22.022
α-D-galactose	1a2e3e4a	2.332	−24.499	−22.167
α-D-talose	1a2a3e4a	2.316	−24.542	−22.226
α-D-mannose	1a2a3e4e	2.338	−24.736	−22.398
β-D-gulose	1e2e3a4a	2.323	−24.810	−22.487
β-D-altrose	1e2a3a4e	2.350	−24.867	−22.517
β-D-idose	1e2a3a4a	2.335	−24.918	−22.583
β-D-galactose	1e2e3e4a	2.344	−24.969	−22.625
α-D-gulose	1a2e3a4a	2.316	−25.038	−22.722
β-D-mannose	1e2a3e4e	2.358	−25.194	−22.837
α-D-allose	1a2e3a4e	2.340	−25.385	−23.045
α-D-altrose	1a2a3a4e	2.339	−25.626	−23.287
α-D-glucose	1a2e3e4e	2.351	−25.699	−23.348
β-D-allose	1a2e3a4e	2.358	−26.251	−23.893
β-D-glucose	1e2e3e4e	2.364	−26.589	−24.225

as the number of axial hydroxyls increases, there is a greater probability that stronger cis-vicinal and syndiaxial intramolecular H-bonds will be present. The results of ANOVA confirm the significance of the syndiaxial OH-1/3 interaction as well as the OH-4 group which is able to H-bond with OH-6. When these groups are axial, the surface of the sugar molecule, in effect, becomes less multipolar, and therefore more hydrophobic, to the solvent as a result of its decreased ability to form solute−solvent H-bonds.

The approximate free energy of solvation (Table 2) reflects how changes in the partial charge distribution at the molecular surface, and consequently the electrostatic field surrounding the molecular surface, affect solute hydration. Axial configuration of hydroxyls, especially at OH-2 and OH-4, is associated with a more positive (less favorable) free energy of solvation. Positive (blue) and negative (red) electrostatic field isosurface contours for a representative series of stereoisomers are displayed in Figure 4 to illustrate how partial charge impacts the surrounding environment. The sugars were chosen for a progressive conversion of hydroxyls 4, 2, and 3 from equatorial to axial configuration: α-glucose, α-galactose, α-talose, and α-idose. Sugars with both OH-2 and OH-4 in axial configuration (α-talose and α-idose) are able to form a syndiaxial intramolecular H-bond. As a result, these sugars have a relatively less complex (less multipolar) isopotential surface than α-glucose (OH-2 and OH-4 equatorial) and α-galactose (OH-2 equatorial, OH-4 axial). In α-talose and α-idose, the sugar faces are dominated by one potential surface rather than a mixture of positive and negative isopotentials. The impact of the electric field generated by the partial charge distribution on water structure is illustrated for these same four sugars in Figure 5.

The results above illustrate how hydroxyl orientation influences the surface properties of aldohexopyranose stereoisomers. The effect of changes in the surface properties of these stereoisomers on hydration can be monitored by analyzing the influence of particular hydroxyls and their H-bond interactions on water structure. As will be shown, the OH-4 group as well as the OH-2/4 and OH-1/3 interactions are important factors influencing water structure.

B. OH-4 Plays a Pivotal Role in Hydration as a Central Component of Intramolecular H-Bond Networks. Analysis of water−water H-bond angle distributions demonstrates the importance of the OH-4 position. As evidenced by higher A1/A2 ratios and lower average H-bond angles (Table 3), axial configuration of the OH-4 group induces relatively more nonpolar-like structure of surrounding water molecules; in other words, water molecules solvating polar groups (OH−OH) are less distorted and have more linear H-bond angles when the OH-4 group is axial. To understand the importance of the OH-4 group and its effect on water structure, one must first understand the nature of the H-bond networks this group forms.

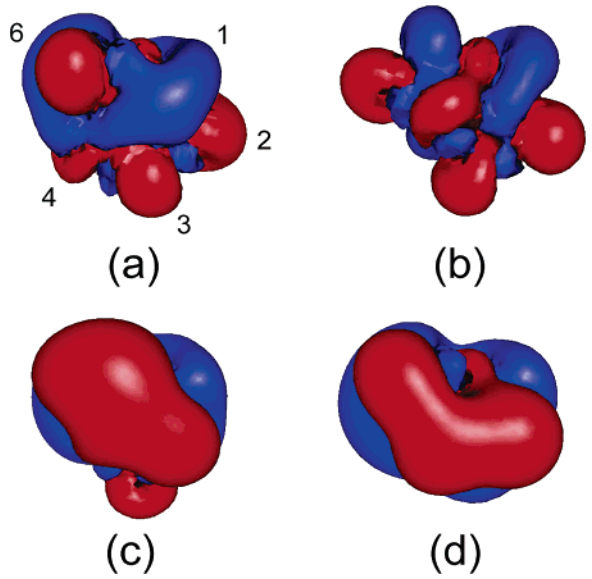

Figure 4. Positive (blue) and negative (red) electrostatic field isosurface contours (0.25 kT/e) for α-glucose (a), α-galactose (b), α-talose (c), and α-idose (d). For orientation, hydroxyl positions are labeled in the first sugar.

Previous studies of aldohexopyranose rotamer distributions have implicated the OH-4 group as an essential component in the formation of H-bond networks utilizing the OH-6 group.[5,31] Since the OH-6 group is freely rotating, a number of arrangements are possible between this group and OH-4. Quantum mechanical simulations of pyranose derivatives have shown that, in solution, a gauche-trans (gt) arrangement of OH-4 and OH-6 groups around the C5−C6 bond is dominant in both gluco- and galactopyranosides.[31] The gt rotamer, in which the OH-6 group is free from intramolecular H-bonding, is estimated to account for greater than 50% of the total rotamer distribution. The rest of the rotamer distribution is composed of a mix of gauche-gauche (gg) and trans-gauche (tg) rotamers. Sugars with an OH-4 equatorial group, as is present in glucopyranosides, form internal H-bonds between OH-4 and OH-6 only when in tg orientation. This orientation is estimated to compose 10−20% of the total rotamer population. However, sugars with an axial OH-4 group can form H-bonds between OH-4 and OH-6 groups when in either tg or gg orientation—in total, 30−50% of the rotamer population. Therefore, the likelihood of intramolecular H-bonding between OH-4 and OH-6 is increased in aldohexopyranosides with an axial OH-4 group.

In examining the frequency of intramolecular H-bond formation between OH-4 and OH-6 in our simulations, the greater tendency of the axial OH-4 to H-bond with OH-6 was confirmed. However, the frequency of intramolecular H-bonding between these two groups is underestimated with respect to the quantum mechanics-based findings described above. In sugars with an axial OH-4 group, such as galactopyranosides, H-bonds between OH-4 and OH-6 were present approximately 6% of the time, as opposed to the 30−50% frequency expected from the rotamer distribution studies. For glucopyranosides, or sugars with OH-4 in equatorial configuration, H-bonding between OH-4 and OH-6 was negligible and not the 10−20% frequency expected. Most of the time, the OH-6 group did not form

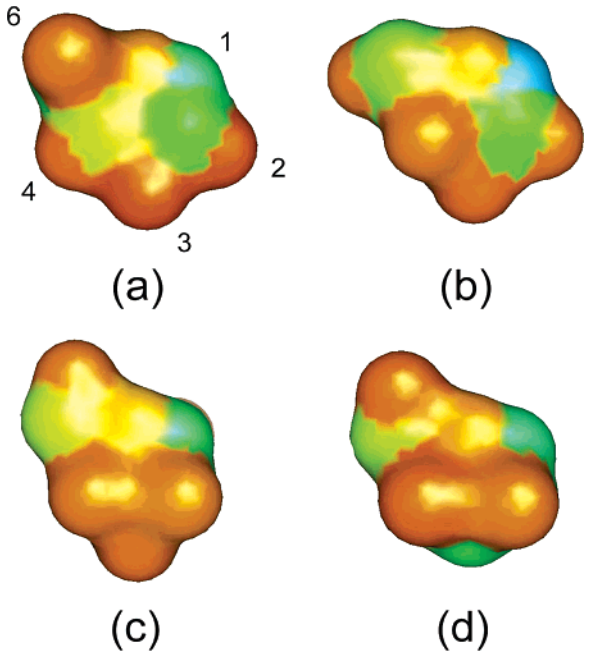

Figure 5. Average water−water H-bond angles associated with α-glucose (a), α-galactose (b), α-talose (c), and α-idose (d); scale ranges from more linear H-bonds (27°, blue) to more bent H-bonds (43°, orange). For orientation, hydroxyl positions are labeled in the first sugar.

intramolecular H-bonds and was instead free to interact with solvent molecules. Therefore, the impact of networks involving the OH-6 group on water structure may be underrepresented in our study. This information should be kept in mind when interpreting results.

Key differences exist between the H-bond networks formed by tg and gg rotamers; these networks differ in both directionality and composition.[5] In the gg rotamer, a terminated H-bond network can form between OH-4 → OH-6 → O-5 (ring oxygen). Termination of this network results in an H-bond center lacking balanced donor and acceptor characteristics. The lack of a free OH hydrogen at position 5 eliminates donor ability of the group. In effect, this makes the H-bond network less able to interact with the water molecules surrounding the sugar in the first solvation shell. As a result, water molecules are preferentially influenced by other water molecules and a more ordered, linear hydration shell forms around the sugar.

In the tg rotamer, H-bonding occurs in the opposite direction of the terminated network described above by forming the OH-6 → OH-4 → OH-3 network. The bond between OH-4 and OH-3 is a weaker cis-vicinal H-bond that occurs when OH-4 is axial and OH-3 is equatorial. This bond is present about 33% of the time when the hydroxyl groups are in this configuration (disregarding the effect of other hydroxyls on the formation of the OH-3/4 H-bond). The weak nature of the cis-vicinal bond has two effects: (1) the OH-3 hydrogen is more able to be an H-bond donor to solvent molecules than to other solute groups, and (2) the strength of the OH-3 donor hydrogen and the OH-4 acceptor oxygen are increased by cooperativity. The strong dual nature of this network allows these hydroxyl groups to more strongly interact with surrounding solvent. The significance of the OH-3/4 interaction is seen in ANOVA of average first-shell water−water H-bond angles as an indirect effect on water structure (Table 4). When OH-4 is axial and OH-3 is equatorial, such as in the above H-bond network, nonpolar groups of the carbohydrate (C−H/C−H) exhibit more polar-like hydration by surrounding water molecules. These results are in contrast to the terminated network, as the water structure surrounding sugars with the nonterminated network exhibits more distorted, less linear H-bonds.

TABLE 3: Low Angle/High Angle Water−Water H-Bond Ratios (A1/A2) for Nonpolar, Polar, and Mixed Class Solute Atom Class, Ranked by Polar Class Ratio

sugar	configuration	polar	nonpolar	mixed	total
α-D-idose	1a2a3a4a	0.746	1.215	0.774	0.785
α-D-talose	1a2a3e4a	0.744	1.143	0.760	0.782
α-D-galactose	1a2e3e4a	0.730	1.198	0.781	0.781
α-D-altrose	1a2a3a4e	0.728	1.158	0.787	0.776
β-D-idose	1e2a3a4a	0.724	1.183	0.794	0.777
α-D-allose	1a2e3a4e	0.722	1.160	0.731	0.765
α-D-gulose	1a2e3a4a	0.721	1.205	0.772	0.770
β-D-talose	1e2a3e4a	0.719	1.072	0.721	0.762
α-D-glucose	1a2e3e4e	0.716	1.238	0.773	0.765
α-D-mannose	1a2a3e4e	0.714	1.208	0.811	0.763
β-D-allose	1a2e3a4e	0.708	1.166	0.769	0.764
β-D-mannose	1e2a3e4e	0.706	1.106	0.717	0.755
β-D-gulose	1e2e3a4a	0.705	1.194	0.776	0.752
β-D-galactose	1e2e3e4a	0.703	1.092	0.748	0.746
β-D-glucose	1e2e3e4e	0.698	1.153	0.776	0.749
β-D-altrose	1e2a3a4e	0.696	1.165	0.797	0.755

Because the OH-3/4 H-bond is cis-vicinal, it is relatively weak compared to syndiaxial interactions. Therefore, in sugars where the OH-2 group is also axial, there may be a preference for an OH-2/4 syndiaxial H-bond over the OH-3/4 vicinal bond. Indeed, in our simulations, the OH-4 → OH-3 H-bond is present 50% of the time when the configuration is OH-4 axial, OH-3 equatorial, and OH-2 equatorial. However, when the OH-2 group is moved from equatorial to axial, where it can H-bond with OH-4, the presence of the OH-4 → OH-3 H-bond drops to only 17%. This line of reasoning explains why α-talose has more nonpolar-like hydration than would be expected for sugars containing the OH-3/4 H-bond (Table 3).

The above analysis of the OH-4 position only limitedly takes into account the effect of other hydroxyl groups. As demonstrated below, other hydroxyls, such as OH-2, affect the directionality and strength of the H-bond network formed by the OH-4 and OH-6 groups.

C. The OH-2 Group Imposes Directionality on Intramolecular H-Bond Networks. In addition to H-bonding with OH-6, OH-4 is able to form an H-bond with OH-2, thus magnifying the effect of intramolecular H-bonding on water structure and solvation. As concluded from ANOVA, H-bonding between OH-2 and OH-4 appears to be the dominant syndiaxial interaction driving water structure surrounding the aldohexopyranose sugars. When both of these groups are axial, our simulations show an intramolecular H-bond present between these groups nearly 90% of the time. This result is indicative of the strength of the syndiaxial interaction, which would in turn have a relatively weak influence on distorting surrounding water structure. As expected, water structure surrounding polar (OH−OH) pairs exhibits relatively more ordered, lower H-bond angles when one or both of the OH-2 and OH-4 groups are in axial configuration (Tables 3 and 4).

The suggestion that OH-2 may have a role in strengthening the effect of H-bond networks involving OH-4 was suggested previously by Galema et al.[32−36] This group used kinetic medium effects,[32,33] partial molar volumes, partial molar isentropic compressibilities, hydration numbers,[35] and partial molar heat capacities[34] to observe how some carbohydrate stereoisomers globally interact with water. Although the axial OH-4 group was the primary group responsible for differences in hydration observed between stereoisomers, the orientation of OH-2 relative to this group influenced the magnitude of the response.[32,37] According to our analysis, stereoisomers with axial hydroxyls

TABLE 4: Significance of Hydroxyl Position Contribution to Selected Responses[a]

	main effects				interactions		
property	OH-1	OH-2	OH-3	OH-4	OH-1/3	OH-2/4	OH-3/4
A1/A2 ratio							
nonpolar							
					n.a.	n.a.	n.a.
polar	0.002	0.047		0.013		0.041	
	0.000	0.038		0.006	n.a.	n.a.	n.a.
mixed					0.030		
					n.a.	n.a.	n.a.
Average Water−Water Hydrogen Bond Angle							
nonpolar	0.005		0.031		0.005		0.007
	0.048				n.a.	n.a.	n.a.
polar	0.002			0.012			
	0.000	0.036		0.003	n.a.	n.a.	n.a.
mixed					0.020		
					n.a.	n.a.	n.a.
Other Properties							
total area	0.003	0.017	0.031	0.001			
	0.001	0.017	0.038	0.000	n.a.	n.a.	n.a.
polar SASA	0.014		0.044	0.000	0.048		
	0.023			0.000	n.a.	n.a.	n.a.
ΔG				0.019			
solvation		0.011		0.001	n.a.	n.a.	n.a.

[a] P values were determined by ANOVA including first and second order interactions (top P value) and first order interactions only (bottom P value) using a significance cutoff of 0.05. Dashed lines indicate P values greater than the cutoff. In cases where values are not applicable, "n.a." is used.

at both OH-2 and OH-4 formed intramolecular hydrogen bonds less able to interact with surrounding water molecules.

Again, it is important to consider the impact of the OH-2 group in terms of the H-bond network. Lopez de la Paz et al. suggest that due to its proximity to the anomeric center, the more acidic OH-2 group is able to impose directionality on and further stabilize the H-bond between OH-4 → OH-6 when forming a syndiaxial H-bond between OH-2 → OH-4.[5] As a result, the terminating network of OH-2 → OH-4 → OH-6 → O-5 would exhibit even stronger acceptor characteristics than if OH-2 were not part of the network.

In our simulations, a preference for the OH-2 → OH-4 intramolecular H-bond over the OH-4 → OH-2 bond was not observed. If the influence of other hydroxyl groups on the interaction between OH-2 and OH-4 is ignored, the frequency of H-bond occurrence is 36% for the OH-2 → OH-4 syndiaxial interaction and 51% for the OH-4 → OH-2 syndiaxial interaction. These results are opposite of what is suggested by Lopez de la Paz et al. Presence of an axial OH-2 group should impose directionality on networks involving OH-4, therefore the OH-2 → OH-4 network should have a higher frequency of occurrence. However, if the impact of OH-6 is considered on the formation of OH-2 → OH-4 → OH-6 and OH-6 → OH-4 → OH-2 networks, the reason for the discrepancy becomes a little more clear. The frequency of occurrence for these networks is 3% and 1%, respectively. While this does not seem like a large difference, one must remember that networks involving OH-6 are most likely underrepresented in our study and that their true frequencies of occurrence may be much higher. Once the impact of OH-6 is included in the analysis, the OH-2 → OH-4 bond is actually more prevalent, as would be expected.

When both OH-2 and OH-4 were axial, the average A1/A2 ratio was significantly higher than the average value exhibited by all other OH-2/4 orientations. In terms of water structure, a higher A1/A2 ratio indicates a water structure more characteristic of hydrophobic solvation. Hydrophobic groups do not perturb water structure to the same degree as polar or charged groups, therefore the structure of solvating water does not deviate greatly from that of bulk water. Interactions between water molecules in this shell dominate, and low-energy, low-angle water−water hydrogen bond angles persist.

These results have implications for understanding the cryoprotective effect of various sugars such as trehalose. Trehalose has no direct intramolecular H-bonds between its hydroxyl groups due to the all-equatorial configuration of its component sugars, two glucose molecules joined by a (1→1) glycosidic bond. The availability of these hydroxyls to H-bond with the solvent leads to a high degree of hydration; trehalose has a larger hydration number than other disaccharides such as maltose and sucrose.[38] As a result, water in the surrounding hydration layers becomes sequestered and is less able to be integrated into the ordered H-bond network of ice. As explained by Branca et al.,[39−41] this destructuring leads to an effective reduction in the amount of "freezable" water and gives trehalose its unique cryoprotective characteristics.

D. The OH-1/3 Interaction is Inefficient in H-Bond Networks but Can Indirectly Influence the Formation of Hydrophobic Patches. Aldohexopyranose sugars can form an additional syndiaxial H-bond through OH-1 and OH-3 groups. While intramolecular H-bonds are formed between axial OH-1 and OH-3 groups nearly 80% of the time, the OH-1/3 intramolecular H-bond does not appear to have the same effect on water structure as the OH-2/4 interaction. In contrast to the effect exhibited by OH-2/4 syndiaxial interactions, which operate through intramolecular H-bonding, the OH-1/3 intramolecular H-bond has an indirect effect on water structure. When both OH-1 and OH-3 groups are equatorial, no intramolecular H-bond is present between these groups and a hydrophobic patch forms on one face of the carbohydrate. The electrostatic potential maps surrounding these hydrophobic patches are shown in Figure 6 and display relatively less multipolar isosurfaces. ANOVA results presented here confirm that it is the hydrophobic patch in OH-1/3 equatorial sugars that is responsible for changes in water structure. When these groups are equatorial, the water structure surrounding nonpolar (C−H/C−H) and mixed atom (O−H/C−H) pairs is more polar-like; that is, H-bond angles between waters in the first solvation shell surrounding these atom groups are larger and more bent.

A possible reason the OH-1/3 interaction does not exhibit strong water structuring effects due to intramolecular H-bonding like the OH-2/4 interaction is that the hydroxyl at position 1 is able to undergo mutarotation when in solution. Mutarotation, or the interconversion of OH-1 between axial and equatorial configurations, results in a mixture of α and β anomers.[42] While mutarotation was not included in our simulations, another factor behind the secondary influence of the OH-1/3 interaction was observed. The hydroxyls at positions 1 and 3 are less able to form intramolecular H-bond networks with OH-6 than OH-2/4. Hydrogen bond distances for two representative sugars; β-talose and α-idose are illustrated in Figure 7. In the sugar β-talose, which contains the syndiaxial groups OH-2 and OH-4, an additional H-bond is able to be formed between OH-4 and the freely rotating OH-6. The syndiaxial groups OH-1 and OH-3 of α-idose are not able to make this extra H-bond contact with OH-6 and would therefore not exhibit the additive effect of a large H-bond network. The limited effect of OH-1/3 on water structure and the formation of hydrophobic patches should not be discounted, however.

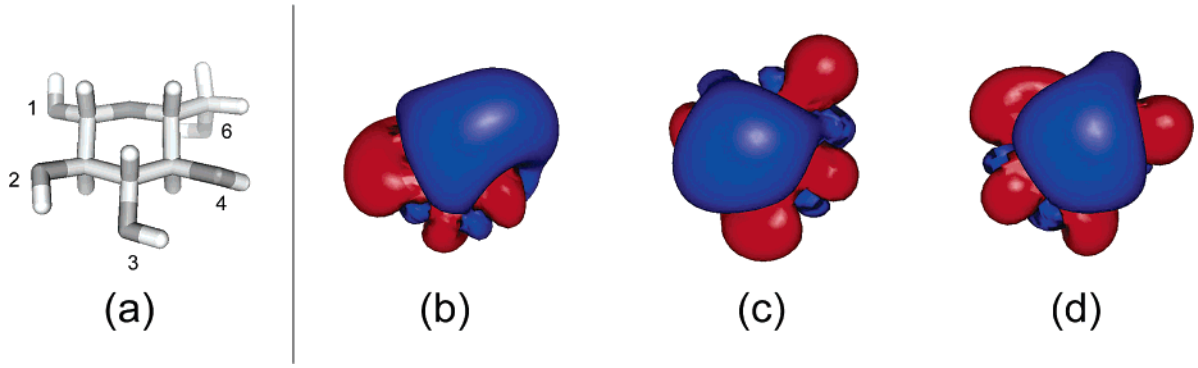

Figure 6. Electrostatic field isosurface contours surrounding the hydrophobic patch of common biological sugars: β-glucose (b), β-mannose (c), and β-galactose (d). Figure 6a is present to show the C−H groups present on the opposite face of these sugars. The figure is slightly offset from face-on view in order to show the vector orientation of these groups. Coloring of b−d follows that of Figure 3.

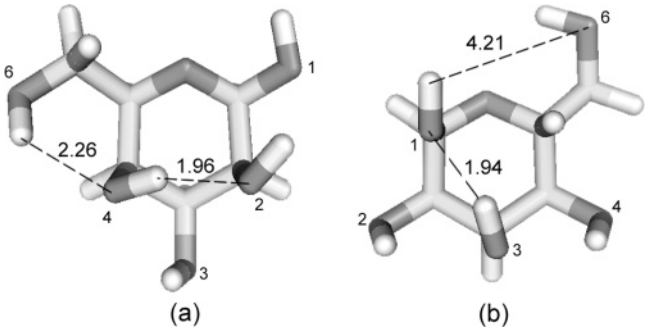

Figure 7. Hydrogen bond distance (Å) between syndiaxial groups β-talose (a) and α-allose (b). Sugars were chosen to illustrate the ability of OH-2/4 and OH-1/3 groups to interact with OH-6. The typical H−O range of carbohydrate intramolecular H-bonds is 1.8 to 2.6 Å.[51]

The hydrophobic patch is important for understanding molecular recognition of carbohydrates by proteins. The nonpolar C−H groups of carbohydrates form patches that are known to interact with aromatic residues of protein side chains in what has been termed a CH-π interaction,[43] van der Waals contact,[44,45] or hydrophobic interaction.[46,47] For example, some lectins use the aromatic side chains of Trp, Tyr, and Phe side chains to readily recognize β-galactose and β-glucose carbohydrates through the hydrophobic patch.[48] Additionally, recent NMR evidence has shown that the hydrophobic patch of galactose analogue methyl β-galactoside interacts with the aromatic benzene, while the mannose analogue methyl α-mannoside, which lacks a hydrophobic patch, does not exhibit these interactions.[49] However, here it should be noted that other interactions, such as cation-carbohydrate binding may be responsible for the α-mannose selectivity of some lectins, such as the calcium-dependent C-type lectins.[50]

IV. Conclusion

Although aldohexopyranose sugars share an identical chemical composition, orientation of individual hydroxyl groups influences the structure of water molecules in the surrounding first solvation layer. The OH-4 group is in a position which allows it to participate in a number of different intramolecular H-bond networks depending on the relative configuration of other groups. When axial, the OH-4 group can hydrogen bond with OH-6 to form a terminated OH-4 → OH-6 → OH-5 network. Because of its imbalanced donor and acceptor characteristics, this network interacts poorly with water and leads to more nonpolar-like hydration surrounding its hydroxyl groups. The axial OH-4 group can also interact with an equatorial OH-3 to form the free-ended OH-6 → OH-4 → OH-3 network. This network influences water structure surrounding the sugar indirectly; that is, water structure surrounding typically nonpolar portions of the molecule (the C−H groups) actually exhibits relatively more polar-like hydration. The OH-2 group, when axial, can induce changes in the networks formed by the axial OH-4 group. This is a result of the strong syndiaxial intramolecular H-bond formed between the OH-2 and OH-4 groups. Presence of the axial OH-2 group can decrease the occurrence of the OH-6 → OH-4 → OH-3 network in favor of networks involving OH-2, OH-4, and OH-6. Additionally, there is some evidence that an axial OH-2 supports directionality of these networks, influencing formation of OH-2 → OH-4 → OH-6 over OH-6 → OH-4 → OH-2. In any case, these strongly H-bonded networks exhibit more nonpolar-like hydration around their hydroxyl groups. Finally, while axial OH-1 and OH-3 are able to form a strong syndiaxial intramolecular H-bond as well, networks formed by these two groups do not have the same effect on water structure as those involving OH-2 and OH-4. The OH-1 and OH-3 groups have only an indirect effect on water structure; when these groups are equatorial, a hydrophobic patch is formed by C−H groups on one face of the sugar. However, the water structure surrounding this patch is actually relatively more polar-like than that observed when the OH-1 and OH-3 are in configurations that do not support patch formation.

It is interesting that the monosaccharides common to biology are those containing both a hydrophobic patch and limited intramolecular H-bonding; namely, glucose, galactose, and mannose. For example, examination of the mucin-type O-linked oligosaccharides implicated in immunological recognition and signal transduction show that the most common monosaccharide components are glucose- and galactose-based sugars and analogues.[1] These carbohydrates display electrostatic potential surfaces with regions of varying complexity; that is, one face of the sugar appears to have a more multipolar presentation to solvent than the other. As a result, the hydration of these two faces in terms of water structure would also differ correspondingly. This arrangement would allow these sugars to be effectively solvated while also having properties conducive to molecular recognition and cryoprotection.

Acknowledgment. This project was supported by the National Research Initiative of the USDA Cooperative State Research, Education and Extension Service, grant number 2005-35503-16151. Support from the NSF (MCB02-35440) for K.A.S. is greatly acknowledged. The authors thank Dr. Ninad Prabhu and Ms. Qingyi Yang for discussions regarding molec-

ular dynamics simulations, electrostatics, and solvation energy calculations and Mr. Nathaniel Nucci for discussions regarding water structure.

References and Notes

(1) Van den Steen, P.; Rudd, P. M.; Dwek, R. A.; Opdenakker, G. *Crit. Rev. Biochem. Mol. Biol.* **1998**, *33*, 151.
(2) Varki, A. *Glycobiology* **1993**, *3*, 97.
(3) Harding, M. M.; Anderberg, P. I.; Haymet, A. D. J. *Eur. J. Biochem.* **2003**, *270*, 1381.
(4) Frank, H. S.; Yen, W. Y. *Discuss. Faraday Soc.* **1957**, *24*, 133.
(5) Lopez de la Paz, M.; Ellis, G.; Perez, M.; Perkins, J.; Jimenez-Barbero, J.; Vicent, C. *Eur. J. Org. Chem.* **2002**, 840.
(6) Crowe, J. H.; Crowe, L. M.; Carpenter, J. F.; Aurell Wistrom, C. *Biochem. J.* **1987**, *242*, 1.
(7) Denisov, V. P.; Jonsson, B.-H.; Halle, B. *Nat. Struct. Biol.* **1999**, *6*, 253.
(8) Svergun, D. I.; Richard, S.; Koch, M. H. J.; Sayers, Z.; Kuprin, S.; Zaccai, G. *Proc. Natl. Acad. Sci. U.S.A.* **1998**, *95*, 2267.
(9) Chalikian, T. V. *J. Phys. Chem. B* **2001**, *105*, 12566.
(10) Liu, Q.; Brady, J. W. *J. Phys. Chem. B* **1997**, *101*, 1317.
(11) Sharp, K. A.; Madan, B. *J. Phys. Chem. B* **1997**, *101*, 4343.
(12) Madan, B.; Sharp, K. A. *Biophys. Chem.* **1999**, *78*, 33.
(13) Madan, B.; Sharp, K. A. *J. Phys. Chem.* **1996**, *100*, 7713.
(14) Gallagher, K. R.; Sharp, K. A. *J. Am. Chem. Soc.* **2003**, *125*, 9853.
(15) Ma, B.; Schaefer, H. F., III; Allinger, N. L. *J. Am. Chem. Soc.* **1998**, *120*, 3411.
(16) Jorgensen, W. L.; Chandrasekhar, J.; Madura, J. D.; Impey, R. W.; Klein, M. L. *J. Chem. Phys.* **1983**, *79*, 926.
(17) Brooks, B. R.; Bruccolcri, R. E.; Olafson, B. D.; States, D. J.; Swaminathan, S.; Karplus, M. *J. Comput. Chem.* **1983**, *4*, 187.
(18) Kuttel, M.; Brady, J. W.; Naidoo, K. J. *J. Comput. Chem.* **2002**, *23*, 1236.
(19) Nose, S. *J. Chem. Phys.* **1984**, *81*, 511.
(20) Nose, S. *Mol. Phys.* **1984**, *52*, 255.
(21) Hoover, W. G. *Phys. Rev. A* **1985**, *31*, 1695.
(22) Ryckaert, J.-P.; Ciccotti, G.; Berendsen, H. J. C. *J. Comput. Chem.* **1977**, *23*, 327.
(23) Gallagher, K. R.; Sharp, K. A. *Biophys. Chem.* **2003**, *105*, 195.
(24) Chelli, R.; Procacci, P.; Cardini, G.; Califano, S. *Phys. Chem. Chem. Phys.* **1999**, *1*, 879.
(25) Yang, Q.; Sharp, K. A., personal communication.
(26) Sharp, K. A. *Biopolymers* **1995**, *36*, 227.
(27) Sitkoff, D.; Sharp, K. A.; Honig, B. *J. Phys. Chem.* **1994**, *98*, 1978.
(28) Sridharan, S.; Nicholls, A.; Sharp, K. A. *J. Comput. Chem.* **1995**, *16*, 1038.
(29) DeLano, W. L. The PyMOL Molecular Graphics System; 0.97 ed.; DeLano Scientific LLC: San Carlos, CA.
(30) Schmidt, R. K.; Karplus, M.; Brady, J. W. *J. Am. Chem. Soc.* **1996**, *118*, 541.
(31) Tvaroska, I.; Taravel, F. R.; Utille, J. P.; Carver, J. P. *Carbohydrate Res.* **2002**, *337*, 353.
(32) Galema, S. A.; Blandamer, M. J.; Engberts, J. B. F. N. *J. Am. Chem. Soc.* **1990**, *112*, 9665.
(33) Galema, S. A.; Blandamer, M. J.; Engberts, J. B. F. N. *J. Org. Chem.* **1992**, *57*, 1995.
(34) Galema, S. A.; Engberts, J. B. F. N.; Hoeiland, H.; Foerland, G. M. *J. Phys. Chem.* **1993**, *97*, 6885.
(35) Galema, S. A.; Hoeiland, H. *J. Phys. Chem.* **1991**, *95*, 5321.
(36) Galema, S. A.; Howard, E.; Engberts, J. B. F. N.; Grigera, J. R. *Carbohydrate Res.* **1994**, *265*, 215.
(37) Chalikian, T. V. *J. Phys. Chem. B* **1998**, *102*, 6921.
(38) Lerbret, A.; Bordat, P.; Affouard, F.; Guinet, Y.; Hedoux, A.; Paccou, L.; Prevost, D.; Descamps, M. *Carbohydrate Res.* **2005**, *340*, 881.
(39) Branca, C.; Magazu, S.; Maisano, G.; Bennington, S. M.; Fak, B. *J. Phys. Chem. B* **2003**, *107*, 1444.
(40) Branca, C.; Magazu, S.; Maisano, G.; Migliardo, P. *J. Chem. Phys.* **1999**, *111*, 281.
(41) Branca, C.; Magazu, S.; Maisano, G.; Migliardo, P. *J. Phys. Chem. B* **1999**, *103*, 1347.
(42) Angyal, S. J.; Pickles, V. A. *Aust. J. Chem.* **1972**, *25*, 1695.
(43) Nishio, M.; Umezawa, Y.; Hirota, M.; Takeuchi, Y. *Tetrahedron* **1995**, *51*, 8665.
(44) Quiocho, F. A. *Pure Appl. Chem.* **1989**, *61*, 1293.
(45) Toone, E. J. *Annu. Rev. Biochem.* **1994**, *65*, 441.
(46) Sundari, C. S.; Balasubramanian, D. *Prog. Biophys. Mol. Biol.* **1997**, *67*, 183.
(47) Elgavish, S.; Shaanan, B. *Trends Biochem. Sci.* **1997**, *22*, 462.
(48) Sujatha, M. S.; Sasidhar, Y. U.; Balaji, P. V. *Protein Sci.* **2004**, *13*, 2502.
(49) Fernandez-Alonso, M. d. C.; Canada, F. J.; Jimenez-Barbero, J.; Cuevas, G. *J. Am. Chem. Soc.* **2005**, *127*, 7379.
(50) McGreal, E. P.; Miller, J. L.; Gordon, S. *Curr. Opin. Immunol.* **2005**, *17*, 18.
(51) Jeffrey, G. A. *An Introduction to Hydrogen Bonding*; Oxford University: Oxford, 1997.